The Climatology of Blocking in a Numerical Forecast Model

JEFFREY L. ANDERSON

Climate Analysis Center/National Meteorological Center, Washington, D.C.

(Manuscript received 22 April 1992, in final form 5 August 1992)

ABSTRACT

An objective criterion for identifying blocking events is applied to a ten-year climate run of the National Meteorological Center's Medium-Range Forecast Model (MRF) and to observations. The climatology of blocking in the ten-year run is found to be somewhat realistic in the Northern Hemisphere, although when averaged over all longitudes and seasons a general lack of blocking is found. Previous studies have suggested that numerical models are incapable of producing realistic numbers of blocks, however, the ten-year model run is able to produce realistic numbers of blocks for selected geographic regions and seasons. In these regions, blocks are found to persist longer than observed blocking events. The ten-year run of the model is also able to reproduce the average longitudinal extent and motion of the observed blocks. These results suggest that the MRF is able to generate and persist realistic blocks, but only at longitudes and seasons for which the underlying model climate is conducive. In the Southern Hemisphere, the ten-year run blocking climatology is considerably less realistic. The appearance of "transient" blocking events in the model distinguishes it from the Southern Hemisphere observations and from the Northern Hemisphere.

A set of 60-day forecasts by the MRF is used to evaluate the evolution of the model blocking climatology with lead time (blocking climate drift) for a 90-day period in autumn of 1990. Although the ten-year run and observed blocking climates are quite similar at most longitudes at this time of year, it is found that blocking almost entirely disappears from the model forecasts at lead times of approximately 10 days before reappearing at leads greater than 15 days. It is argued that this lack of a direct transition between observed and model blocking climates is the result of a drift in the underlying climate (for example, the positions of the jet streams) in the MRF forecasts. If so, the climate drift of the MRF must be further reduced in order to produce more accurate medium-range forecasts of blocking events.

1. Introduction

Blocking events in the atmosphere can have prolonged and significant impacts upon surface climate because of their large amplitude and persistent nature. The same behavior has made blocking events one of the primary targets of medium-range forecast models. An assessment of the ability of a modern numerical weather prediction (NWP) model to forecast blocking events is therefore of great interest as a gauge of the current level of skill in medium-range forecasts.

Blocking events have been one of the most heavily studied atmospheric phenomena since their initial documentation by Rex (1950). Since that time, a variety of studies have been published dealing with the climatology and dynamics of observed blocks. Many earlier studies, for instance Dole and Gordon (1983), concentrated on the Northern Hemisphere wintertime where Rex's "classical" blocks are found. Other studies went on to document the climatology of Northern Hemisphere blocks throughout the year. Unfortunately, the difficulties involved in formulating a universally acceptable objective criterion for identifying blocks has led to the use of many different methods of defining blocks. Lejenäs and Økland (1983) produced an annual climatology of Northern Hemisphere blocks using the midlatitude meridional height gradient as a criterion. Dole and Gordon (1983), followed by Shukla and Mo (1983), performed a similar study but used long-lived anomalies exceeding a threshold value to identify blocks.

A number of observational studies have recently documented many details of the Southern Hemisphere climate (Trenberth 1991). Because Southern Hemisphere blocks have smaller amplitudes and are apparently less common than their Northern Hemisphere counterparts (Trenberth and Mo 1985), these blocks have received relatively little direct attention. Case studies like that of Berberry et al. (1989) have documented some of the Southern Hemisphere blocking regions. Southern Hemisphere blocks have also received significant indirect attention in papers on possible multiple equilibria (Hansen and Sutera 1991), where a relatively blocked flow may be associated with one of the observed equilibria. In addition to the studies of the climatology of blocking, a number of studies have also examined the dynamics responsible for in-

Corresponding author address: Jeffrey L. Anderson, Geophysical Fluid Dynamics Laboratory, Princeton University, P.O. Box 308, Princeton, NJ 08542.

dividual blocking events (Illari 1984; Mullen 1986; Mak 1991).

A question of great interest in the study of blocks is the ability of general circulation models (GCMs) and NWP models to form and persist blocking events. The primary reason is that these models must be able to simulate blocking events in order to produce reasonable forecasts of the atmosphere. In order to make relatively long lead forecasts, the model "climate" must be able to persist and form blocks.

Because of the extreme cost of integrating GCMs at resolutions deemed sufficient to resolve blocking, many studies of the climatology of blocking in models have been for "fixed-season" integrations. Blackmon et al. (1986) and Mullen (1986) describe a 1200-day perpetual January run of an R15 version of the NCAR Community Climate Model (CCM). Their model was able to reproduce the preferred blocking regions over the Northern Hemisphere oceans, but was unable to produce a tertiary maximum in blocking over Siberia, the only maximum over land. Mullen (1989) later extended this study to examine the effects of anomalous SSTs on the climatology of blocking. Xu et al. (1990) compared four GCMs for perpetual January and July conditions in the Southern Hemisphere; in general the quality of such models appears to be worse in the Southern than in the Northern Hemisphere. A comparison of two versions of the CCM for perpetual July over the Southern Hemisphere (Hansen et al. 1991) demonstrates how sensitive model climatologies can be to relatively minor model changes. Model runs have also been used to examine the dynamics leading to the formation of individual blocking events (Chen and Shukla 1983).

Long integrations of seasonally varying GCMs have also been undertaken. Chervin (1986) used a 20-year seasonal cycle run of the CCM to examine the purely internal variability of the model. Randell and Williamson (1990) compared the climate of a seven-year run of the CCM to observations. As in many GCMs, the CCM was found to have too little transient kinetic energy in midlatitudes. Even longer runs, for instance, the 100-year run of Houghton et al. (1991) have examined the climate of simpler GCMs.

The short-term evolution of NWP models and their ability to simulate blocking has also received attention. Tibaldi and Molteni (1990) examined seven years of wintertime European Centre for Medium-Range Weather Forecasts (ECMWF) forecasts with lead times out to ten days. They found that the number of blocks predicted by the model decreased rapidly with increasing lead time. The model was progressively less able to form or persist blocks as the lead time increased. The same behavior was found for the NMC Medium-Range Forecast Model (MRF) (Tracton et al. 1989; Tracton 1990). In these studies, dynamical extended-range forecast (DERF) runs of the MRF were made to lead times of 30 days for 108 consecutive Northern Hemisphere winter days. Again, the MRF was unable to form or persist blocks at lead times greater than approximately five days.

The present study investigates the ability of the MRF to forecast blocking events. Blocks are chosen as the quantity of interest primarily because they have become the focus of many studies on extending the range of useful numerical forecasts (Tracton 1990). This study begins by examining the climatology of blocking in a ten-year seasonal cycle run of the MRF. This extends previous results like those of Blackmon et al. (1986) to all seasons and both hemispheres.

The blocking climatology of the model is interesting in its own right, but the evolution of the observed climate toward the model climate, the climate drift of the model, has the most immediate application to numerical prediction. The MRF blocking climate drift is examined for two seasons using a large set of 90-day forecast integrations. This part of the study is similar to the work of Tibaldi and Molteni (1990), but utilizes forecasts with much greater lead times.

The experiments to be presented allow conclusions to be drawn regarding several aspects of the MRF. The quality of the model's climate can be evaluated by a direct comparison with observations. Several studies (Tracton 1990; Tibaldi and Molteni 1990) have questioned the ability of models to form and persist blocks in a realistic fashion. This question can be addressed using the model blocking climatology.

The next section discusses the details of the ten-year MRF run and the observed datasets used in this study. Section 3 develops an objective method that defines a block as a set of midlatitude easterly flow events. Sections 4 and 5 apply the objective method to present observed and model climates of both easterly flow events and blocks. Section 6 examines the evolution of the MRF blocking climatology as a function of lead time using a series of 90-day integrations of the MRF, while section 7 presents conclusions.

2. Data

a. Ten-year run

A ten-year integration of the National Meteorological Center's Medium-Range Forecast Model (MRF) is investigated in the first part of this study. Details of the MRF can be found in Kalnay et al. (1990) and Kanamitsu et al. (1990). The ten-year run uses a T40 version of the model starting from observed conditions on 31 July 1990 and was performed by H. van den Dool, S. Saha, M. Chelliah, Z. Toth, and W. Ebisuzaki at NMC. The version of the MRF used for the ten-year run (and also for the DERF90 experiment discussed in section 6) is a reduced resolution version of the operational MRF in use during 1990; details of this model are documented in White and Caplan (1991). Here, T21 streamfunction fields, produced from vorticity fields at 300, 500, and 700 mb, are examined.

The ten-year run has climatological values updated daily for all boundary conditions; hence, all variability in the model results is either internally generated or forced by the annual cycle. To give a simple measure of the robustness of the results, the ten-year run is also split into two five-year datasets. The degree of similarity between the two five-year sets is the only direct measure of the statistical significance of the results presented here. Other studies of particular aspects of the climate of this ten-year run can be found in Van den Dool and Saha (1993) and Van den Dool et al. (1991).

b. *Observed data*

The ten-year run data is compared to a five-year observed T21 truncation of NMC's global data assimilation system (GDAS) analysis (Kanamitsu 1989), available from 16 May 1986 through 15 May 1991. This dataset was produced by Z. Toth at NMC. Although this is a short period for producing a climatology, the GDAS analyses in the dataset were produced using versions of the MRF that are similar to those used in the ten-year run. Hence, differences between the datasets that might be caused by the use of a different model for the analysis are minimized. Again, data are available in the form of 300-, 500-, and 700-mb streamfunctions.

3. Objective identification of blocking events

Because of the importance of blocks in generating persistent surface weather patterns, a large number of studies have been published dealing with the analysis and forecasting of these events. To use large datasets, it is prerequisite to have an objective method to identify blocks. Dole and Gordon (1983) defined blocks as midlatitude positive height anomalies exceeding a seasonally dependent threshold value for at least seven days. A different approach was taken by Lejenäs and Økland (1983) who defined a blocking index as $Z_{40} - Z_{60}$, where Z_{40} and Z_{60} are the values of the 500-mb height at 40°N and 60°N. A block was assumed to exist if the blocking index was negative at a given longitude. In the study most closely related to the present contribution, blocks in the ECMWF forecast model were studied by Tibaldi and Molteni (1990). They used a modified version of the Lejenäs and Økland criterion in which the difference in heights between several latitudes separated by 20 degrees was examined at each longitude. In addition to a negative value for this blocking index, Tibaldi and Molteni required the gradient of height south of the block to be relatively small in order to exclude large southward displacements of the jet from consideration as blocks.

The lack of agreement on an objective method for identifying blocks is problematic but not surprising. Synopticians appear to have similar difficulty in agreeing on what can be classified as a blocked flow. In this study, a further modified version of the criterion of Lejenäs and Økland is used; the choice of method is predominantly motivated by the data available and the goals of the study. The method used to find blocks is also assumed to define a "block" for the purposes of the remainder of this study. In general, examining a year of data suggests that the majority of the objectively defined blocking events are consistent with synoptic experience. However, this study is purely comparative so an exact relation between blocks as defined here and traditional synoptic blocks is not essential. Instead, the ability of the forecast model to reproduce the observed behavior is of primary importance.

Easterly flow events

The first step in the objective identification of blocks is the identification of easterly flow events. The strength of the maximum easterly midlatitude flow resolved in the T21 data is defined as

$$E = \max_{i=24,29;i<j\leq 30} (\psi_j - \psi_i)$$

ψ_{24} = 37.6° (north or south) streamfunction

ψ_{25} = 43.0°

ψ_{26} = 48.4°

ψ_{27} = 53.7°

ψ_{28} = 59.1°

ψ_{29} = 64.5°

ψ_{30} = 69.8°.

This easterly flow strength can be defined for each longitude of a streamfunction pattern.

The first step toward finding blocks is to attempt to remove those easterly flow events that are not blocks. Many phenomena besides blocking can induce easterly midlatitude flow. Most of these, for instance transient closed cyclones, produce easterly flows that are relatively weak (at least at T21) compared to those found in major blocks. For this reason, a threshold is applied to the easterly flow strength value; only those easterly flows exceeding the threshold are considered. The threshold values are selected empirically to retain all "classical" blocking events while rejecting as many other events as possible. In general, a threshold of 7.5 10^6 m^2 s^{-1} is used for E in the Northern Hemisphere, while 2.5 10^6 m^2 s^{-1} is used in the Southern Hemisphere where both blocks and other events were found to have weaker easterly flows.

Once those easterly flow events below the threshold have been discarded, the remaining events are grouped into blocks. Blocking events are assumed to be composed of sets of spatially and temporally contiguous easterly flow events (Lejenäs and Økland 1983). An easterly flow event at longitude m and day n is assumed

to belong to the same block as any easterly flow events found at the neighboring longitude/day pairs $(m/n + 1, m/n - 1, m + 1/n, m - 1/n)$. Once this grouping process is complete, all groups that consist of easterly flow events from only a single day are discarded (blocking events are generally regarded as being considerably more persistent than a single day), and all the remaining groups are considered to represent blocking events.

The position of a block at a given day is defined as the longitude of the centroid of the constituent easterly flow events from that day (note that it is possible to have "holes" in a block so that it is not composed of longitudinally contiguous easterly flow events on a given day). For each block, the following information is available: 1) the longitude of the block at its first and last day; 2) the average and maximum strength of easterly flow events, E, for each individual constituent day and for the block as a whole; 3) the longitudinal width (number of easterly flow components) composing the block on each day; 4) the duration of the block in days. In addition, it is possible to compute other fields, for instance the speed of a block, from the stored information.

4. Easterly flow events

Before attempting to compare the climatology of blocking in the model and the observations, it is instructive to examine the relative number of midlatitude easterly flow events. As noted in the last section, these easterly events are a superset of the events that compose blocks.

Easterly flow events are compared using contour plots of the frequency of occurrence (number of days with easterly flow divided by total days) of such events as a function of longitude and time of year (Figs. 1 and 2). The 64 longitude points of the T21 Gaussian grid are the horizontal axis. Reverse-flow events are placed into 12 bins by the month of their occurrence on the vertical axis. The plots are contoured every 0.1 with light stippling above 0.1 and heavy stippling above 0.3.

a. Northern Hemisphere

Figure 1 displays the frequency of easterly flow events exceeding a threshold of 7.5×10^6 m^2 s^{-1} in the Northern Hemisphere for the observations and for the first and second halves of the ten-year run. The ten-year run does a reasonable job reproducing the seasonal cycle of frequency including the observed winter maxima over the Pacific and Atlantic Oceans. However, with the exception of the wintertime oceanic maxima, the frequency of easterly flow produced by the model is too small at all longitudes and seasons. As found in previous studies (Tibaldi and Molteni 1990), the model's center over the Atlantic is somewhat too far

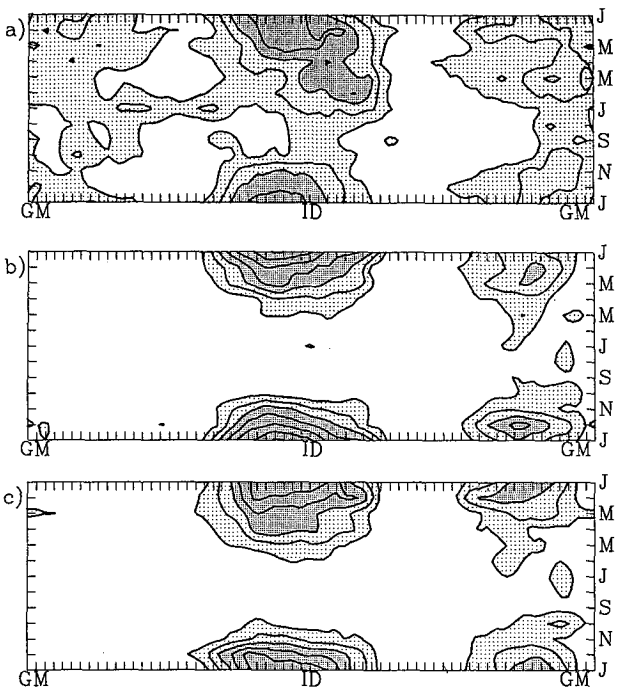

FIG. 1. Frequency of Northern Hemisphere days with easterly flow index exceeding 7.5 10^6 m^2 s^{-1} for (a) observations, and (b) first, and (c) second halves of the ten-year run with contour interval of 0.1. Regions greater than 0.1 are lightly stippled while regions greater than 0.3 have heavy stippling. Horizontal axis is longitude and vertical is month. The international date line is noted as ID and the Greenwich meridian as GM.

west. The ten-year run does not reproduce the weak winter maximum to the east of 45°E. This is consistent with the inability of previous GCM runs to reproduce the observed Siberian blocking maximum (Blackmon et al. 1986), although the MRF does have a low-frequency standard deviation maximum over northern Siberia (Barnston and van den Dool 1993). The model is also unable to capture the summer frequency maximum that extends across most of Eurasia into the Pacific.

The robustness of the ten-year run climate can be examined by comparing the easterly flow frequency in the two five-year halves (Figs. 1b and 1c). The two halves are extremely similar, especially when compared to the much larger differences between them and the observed frequency. This suggests that the ten-year dataset is sufficient to resolve the significant differences between the observed and ten-year run climates. Similar agreement is found for easterly flow frequency in the two halves of the ten-year run at all other levels and thresholds studied and in the Southern Hemisphere.

b. Southern Hemisphere

Figure 2 displays the frequency of easterly flow events exceeding a threshold of 2.5×10^6 m^2 s^{-1} in the South-

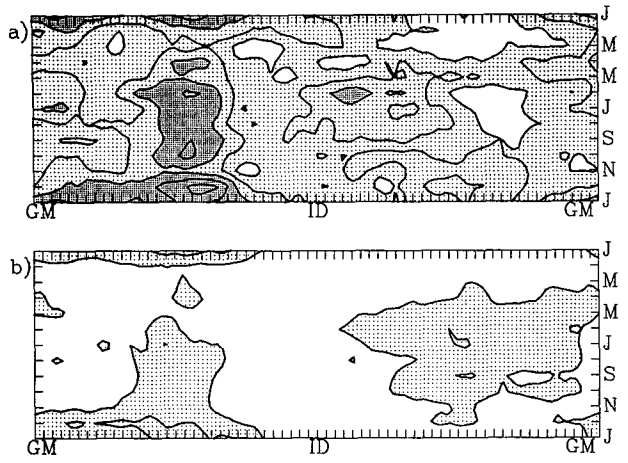

FIG. 2. Frequency of Southern Hemisphere days with easterly flow index exceeding 2.5 10^6 m^2 s^{-1} for (a) observations and (b) ten-year run. Details of presentation are as in Fig. 1.

ern Hemisphere for the observations and for the ten-year run. The observations are dominated by a southern summer maximum throughout the eastern hemisphere, a winter maximum at about 100°E, and a weaker winter maximum around 160°W. The ten-year run produces far too few reverse-flow events although it does produce a semblance of all three maxima. The ten-year summer maxima in the western hemisphere is too far east and too broad.

c. *Additional pressure levels and thresholds*

The easterly flow frequency of the ten-year run and the observations have also been compared for 300 and 700 mb, and for a variety of thresholds ranging from 0 to 1.0 ($\times 10^7$ m^2 s^{-1}) in both hemispheres. The change in threshold has little effect on the general patterns, although the local frequencies obviously increase as the threshold is reduced. The 700- and 300-mb levels also produce generally similar patterns although details of some regions of low-easterly flow frequency are level-dependent.

5. Blocking events

In this section, the climatology of the blocking events defined in section 3 is compared for the ten-year run and the observations. First, the annual mean hemispheric distributions of blocks are examined briefly. Then, a monthly climatology similar to that just discussed for easterly flow events is presented separately for each hemisphere.

a. *Hemispheric blocking summaries*

Figure 3 displays histograms of the number of blocks lasting n days or longer in the ten-year run and the observations (the observed numbers are doubled so that the comparison is for ten years). The most obvious result agrees with those from previous studies (Blackmon et al. 1986; Tibaldi and Molteni 1990); the total number of blocking events produced by the model is insufficient. In the Northern Hemisphere, the number of extremely long-lived blocks is relatively good in the ten-year run; however, as the lifetime decreases, the number of model blocks becomes a progressively smaller percentage of the observed. The number of blocks that live exactly n days can also be determined from the histogram as the difference in number between days n and $n + 1$. Ten-year blocks that have lasted n days are more likely to persist for an additional day than are observed blocks in the Northern Hemisphere for all values of n. This indicates that the ten-year run is unable to produce as many blocks as are observed; however, the blocks it does produce are longer-lived than those in the observations. This is an apparent contradiction to the results of several earlier studies that suggest that models are unable to produce sufficiently persistent blocks (Tibaldi and Molteni 1990; Tracton 1990). This will be discussed more in section 6.

Figure 3b for the Southern Hemisphere indicates a different model behavior. Although the ten-year run is able to produce almost as many short-lived blocks as are observed, the relative number of ten-year blocks decreases rapidly until it is essentially zero by 15 days. Hence, in the Southern Hemisphere, the ten-year run is able to produce blocks at almost the observed rate, but these blocks are not sufficiently persistent.

The relationship between maximum block strength and duration of a blocking event is also of interest. Figure 4 plots the scatter of the duration of blocking events versus the maximum strength of any easterly flow event that is part of the block for the ten-year run and the observations in the Northern Hemisphere. It is important to remember that the observed scatter is for five years while the model results are for ten years. The first thing to note is that the average maximum strength of model blocks is considerably less than that for the observations. Apparently the ten-year run is unable to produce blocks with the same strength as the stronger observed blocks. On the other hand, comparing the average maximum strength for each duration demonstrates that model blocks of a given strength tend to persist longer than their observed counterparts. The inability of GCMs to generate flows with realistic amplitude is well known (Miyakoda et al. 1986; Randel and Williamson 1990); however, the enhanced persistence of weaker blocks in the Northern Hemisphere of the model does not appear to have been noted previously.

The relationship between maximum block strength and duration of a blocking event is similar in the Southern Hemisphere (not shown here). The ten-year run is unable to produce blocks with maximum easterly flow values that are nearly as large as those observed.

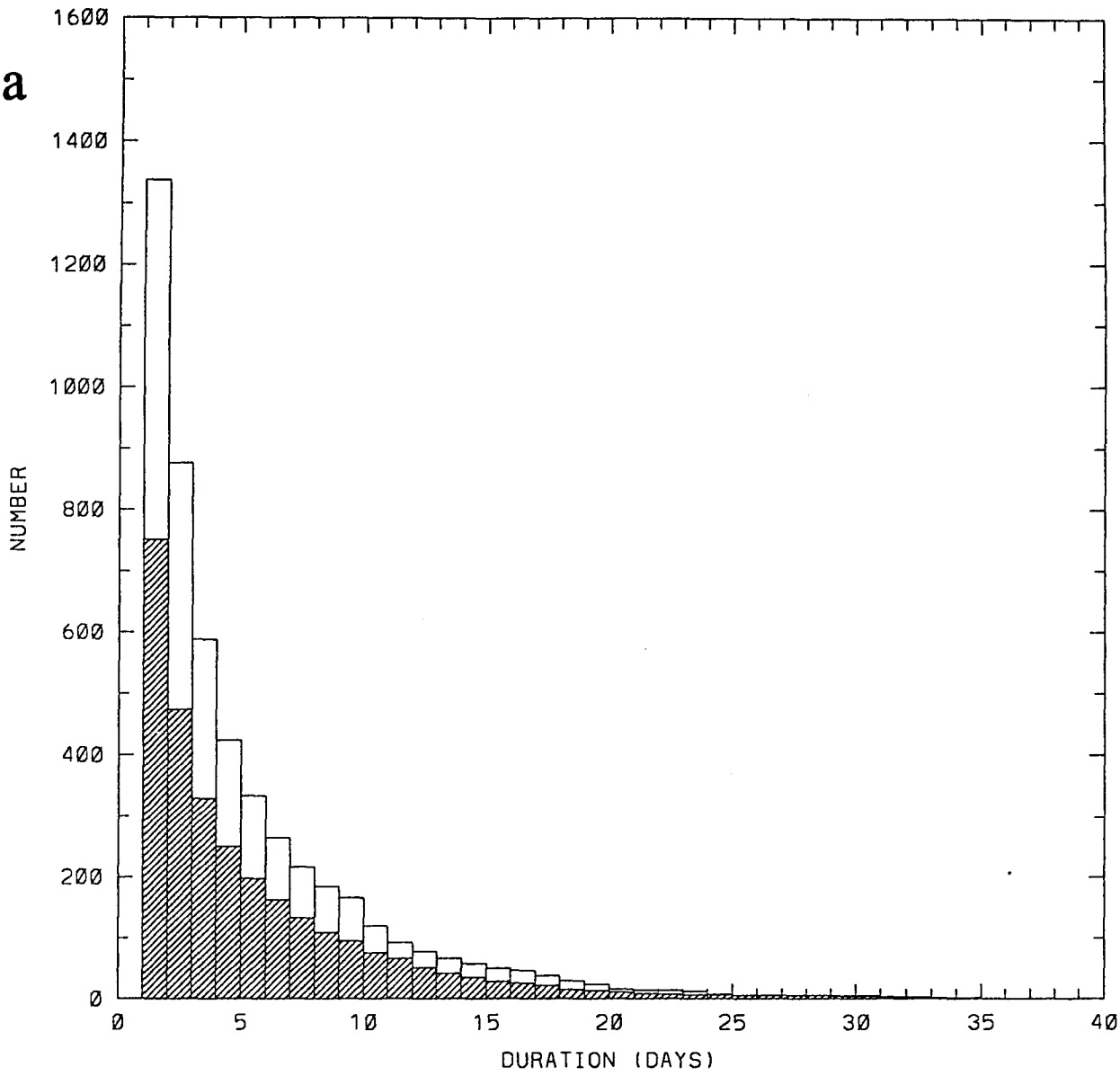

FIG. 3. Histogram of number of observed (unshaded) and ten-year run (shaded) blocks that last at least n days for the (a) Northern Hemisphere and (b) Southern Hemisphere.

As in the Northern Hemisphere, however, ten-year run blocks with a given maximum strength tend to persist longer than observed blocks with similar maximum strengths. Since the number of long-lived Southern Hemisphere ten-year blocks was shown in Fig. 3 to be extremely small, the differences between the ten-year and observed scatterplots for the Southern Hemisphere are considerably more noticeable than those for the Northern Hemisphere shown in Fig. 4.

b. Relating easterly flow and blocking events

Section 4 described the climatology of easterly flow events as a preamble to the present discussion of blocking. There were two reasons for this. First, the easterly flow frequency results are considerably more robust than the blocking results to be presented later due to the much larger number of easterly flow events. Second, it is instructive to compare the blocking and easterly flow events by noting the following relation:

$$\text{east} = \text{number} * \text{duration} * \text{width} + \text{singles}.$$

For stationary blocks, the number of easterly flow events for a given longitude and month is approximately equal to the product of the number of blocks forming, the duration of those blocks, and the average number of easterly flow events associated with each

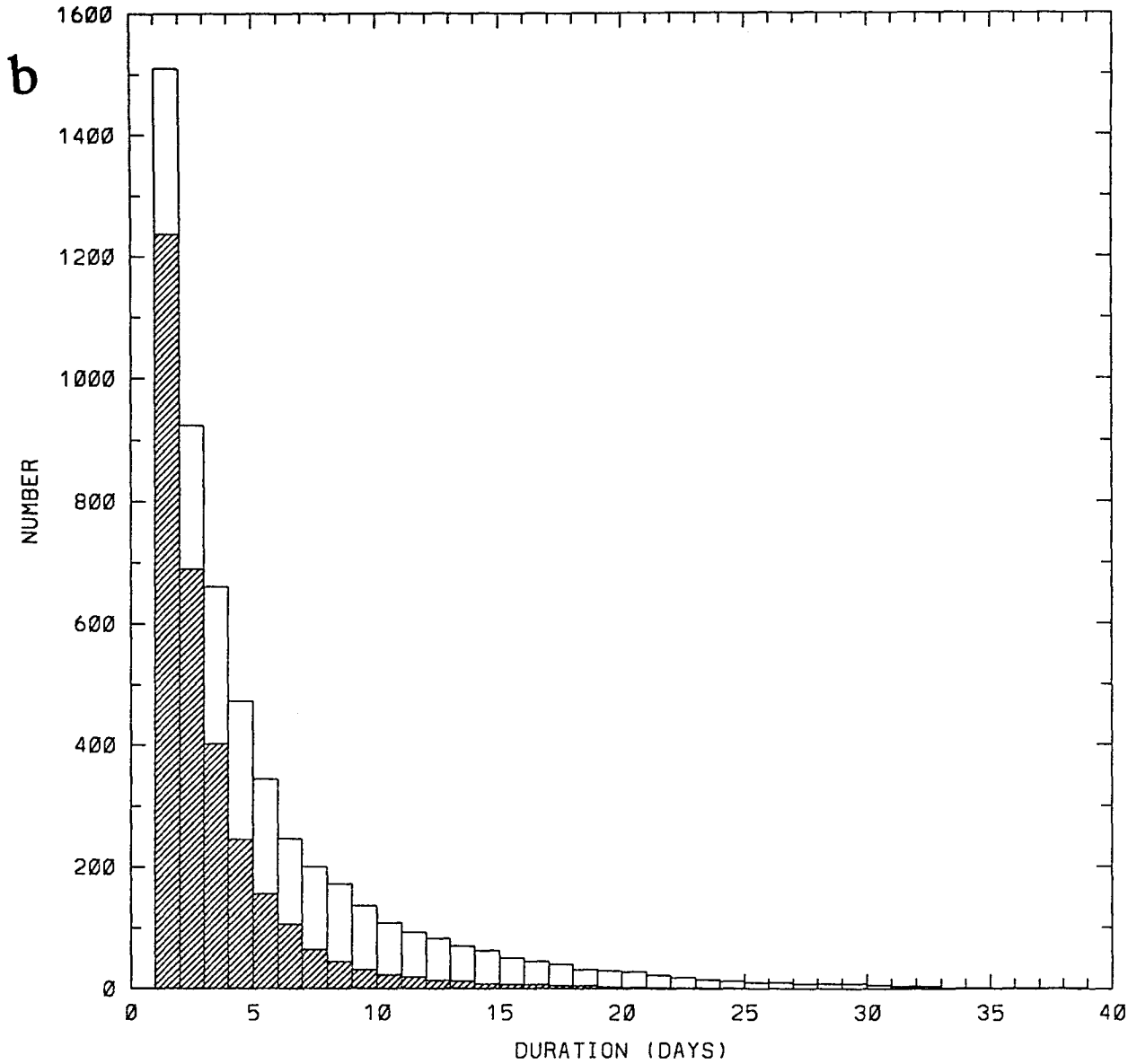

FIG. 3. (*Continued*)

day of the block plus the number of single-day easterly flow events not associated with any block. This framework can be used to compare the section 4 results with those below, especially in the Northern Hemisphere. It is also important in section 6 where easterly flow events must be used as a proxy for blocks.

c. Results

A number of different quantities associated with blocking events will be displayed as functions of longitude and month of the first day of the block. These charts are produced in the same format as the easterly flow frequency charts (Figs. 1 and 2). When the number of blocking events is compared, the number in the observations is multiplied by two to give results for ten years.

The blocking plots are necessarily much noisier than the easterly flow frequency plots because there are many fewer blocks. The unsmoothed plots are too noisy to interpret easily, so the data is smoothed in the longitudinal direction (using a simple seven-point average). Comparisons between the first and second half of the ten-year run are again used to examine the robustness of the results.

The first field discussed is the block width; the average number of easterly flow events per day in a block. This quantity was found to be quite similar in both the

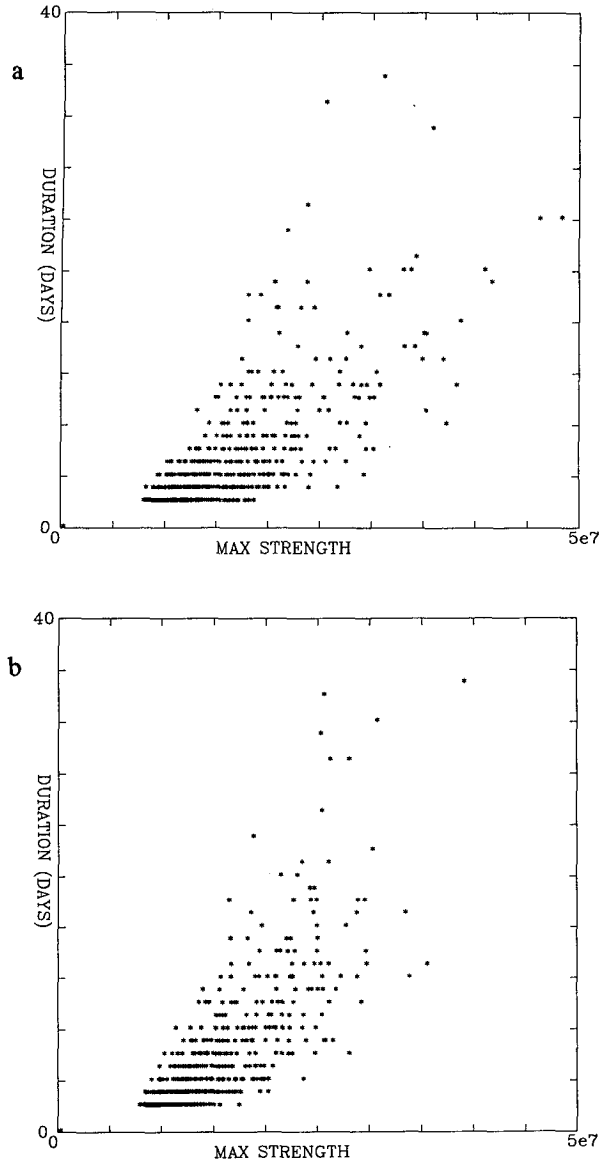

FIG. 4. Scatterplots of the maximum easterly flow strength versus duration for (a) observed and (b) ten-year run blocking events.

ten-year run and observations in both hemispheres. For this reason, the results are not displayed and differences in block width can generally be neglected when comparing the results. The other results are hemispheric-dependent and are discussed separately.

1) NORTHERN HEMISPHERE

Figure 5 shows the number of blocks whose first-day centroid is at a given longitude and month. The observations, Fig. 5a, demonstrate a broad maximum over the Pacific with largest local values in summer and a pair of joined centers over the eastern Atlantic and Europe at all seasons.

Figure 5b and 5c show the same field as Fig. 5a, but for the first and second five years of the ten-year run. The two fields are seen to be reasonably similar, especially when compared to the observed field in Fig. 5a. Apparently, five years is a sufficient period of time to reasonably resolve the differences between the model and observed climate. The degree of similarity between the two halves of the ten-year run was found to be roughly comparable for all the other fields that will be presented here at all levels and in both hemispheres.

The ten-year run of the model, Figs. 5b,c, does a reasonable job reproducing the winter Pacific blocking maximum, but it misses the summer blocks in that region. It has an Atlantic maximum at all seasons, but it is too far west. The maxima over Eurasia are not well represented in the ten-year run.

Figure 6 depicts the average duration of blocks starting at a given longitude and month. The observed pattern is rather noisy, but shows the longest-lived blocks occur in two groups over the Pacific, one in the early winter and the other in the spring. The observed Atlantic and European blocks are considerably more ephemeral than those observed in the Pacific. The very long-lived high-latitude blocks known to occur over Siberia are also represented in the observed duration plot.

The ten-year run block duration is shown in Fig. 6b. The plot is much less noisy than the observed and

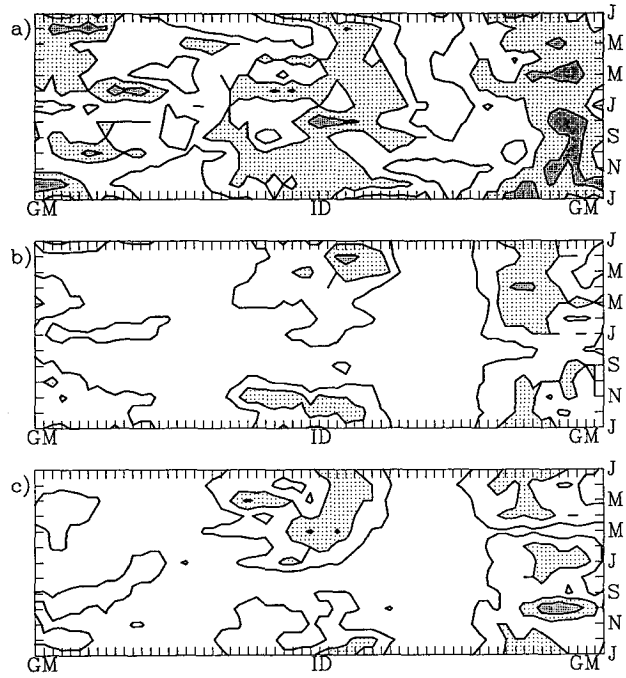

FIG. 5. Number of Northern Hemisphere blocking events formed at a given longitude and month for (a) the observations, (b) the first half of the ten-year run, and (c) the second half of the ten-year run. Contour interval is 1.0 with light stippling for values exceeding 2.0 and dark stippling for values exceeding 3.0.

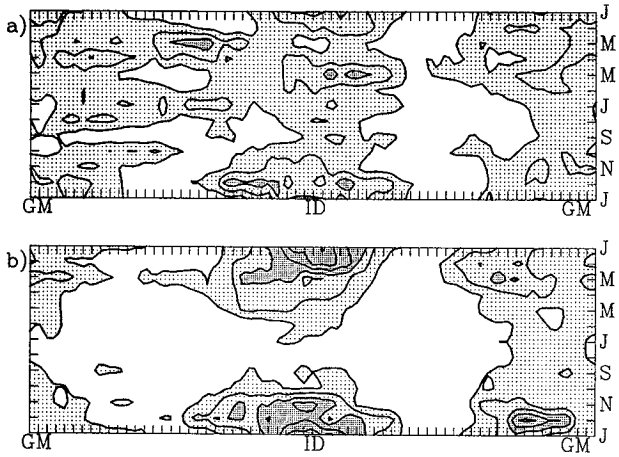

FIG. 6. Average duration in days of (a) observed and (b) ten-year run Northern Hemisphere blocking events. Contour interval is 2.0 with light stippling for values exceeding 2.0 and dark stippling for values exceeding 6.0.

shows that long-lived blocks occur over the Pacific and the Atlantic during the winter season. Over both oceans, the maximum duration values are much larger than the largest seen in the observed data. Apparently, once a block is formed over the wintertime oceans in the model, it is apt to persist for an unusually long time.

Another quantity of interest is the movement of blocks during their lifetimes. For the Northern Hemisphere, plots of both the total movement of blocks, and the speed of blocks (movement/lifetime) show that the ten-year run and the observations are extremely similar (figures not shown). Both show the average block to be essentially stationary throughout its lifetime. Apparently, the model is able to adequately reproduce the nearly stationary behavior of observed blocks.

In addition, this result supports the objective technique being used to identify blocking events. Most other atmospheric phenomena that might be associated with easterly flow events are not observed to be stationary, while blocks are normally nearly stationary throughout their lifetimes. Apparently, at least in the Northern Hemisphere, the objective selection is predominantly locating blocking events.

Northern Hemisphere blocking events have been studied for 300 and 700 mb and for a variety of threshold values. The results are not particularly sensitive to any of these changes. Comparison of the 300-, 500-, and 700-mb results was unable to determine any significant tilt with height of the blocking events, suggesting that these events are either equivalent barotropic or that their tilt with height is small enough that it cannot be resolved by the coarse longitudinal resolution.

An interesting additional experiment involved comparison of an observed blocking climatology with a threshold of 7.5×10^6 m^2 s^{-1} with ten-year run climatologies having thresholds of 5.0×10^6 m^2 s^{-1} and 2.5×10^6 m^2 s^{-1}. Since the ten-year run is incapable of producing sufficiently strong blocks, it is not inconceivable that the only real problem with the model climatology is a consistent lack of strength. However, the comparison of the lower threshold ten-year run results with the standard observed run did not increase the similarity between the two results, and in general, produced a significant degradation in similarity. Apparently a lack of amplitude is not the only failure of the ten-year run. The same results were found for similar experiments in the Southern Hemisphere.

2) SOUTHERN HEMISPHERE

Figure 7 shows the number of Southern Hemisphere observed and ten-year run blocks whose first-day centroid is at a given longitude and month. The most obvious difference is the general lack of block formation anywhere in the ten-year results. The pattern of the ten-year block genesis is also poor. The maximum in the eastern hemisphere occurs at the wrong time of year, and the maxima in the western hemisphere are far too diffuse and in the wrong areas in the ten-year run. The model's blocking climatology in the Southern Hemisphere appears to be far worse than was found for the Northern Hemisphere.

The observed duration of blocks in the Southern Hemisphere is also poorly reproduced by the ten-year run. As already demonstrated in Fig. 3b, most Southern Hemisphere blocks in both the observations and model are short-lived. This is reflected by a widespread background level of block duration just greater than two days for all longitudes and seasons in both the observed and ten-year run (figures not shown). However, there are a number of localized regions in which blocks of

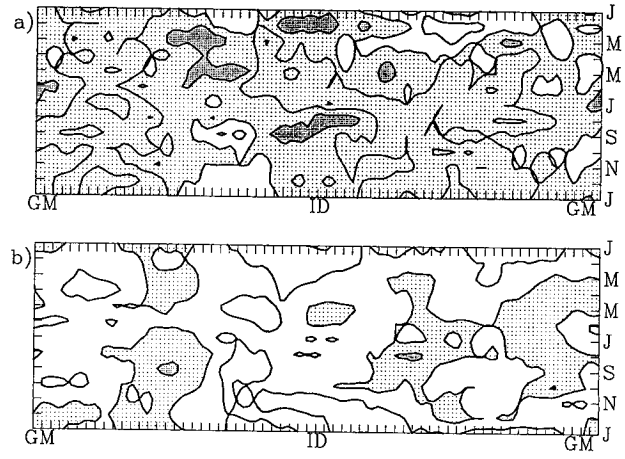

FIG. 7. Number of Southern Hemisphere blocking events formed at a given longitude and month for (a) observations and (b) ten-year run. Details of presentation are as in Fig. 5.

much longer duration are found in the observations, the most notable regions being in Southern Hemisphere winter around 90°E and near 180°. The ten-year run is totally unable to produce these areas of longer average block duration.

Perhaps the most enlightening information about Southern Hemisphere blocking events can be obtained from the average block speed plots shown in Fig. 8. While the Northern Hemisphere blocks are nearly stationary, this is not the case for the Southern Hemisphere. In Fig. 8a, the observed blocks are shown to be relatively transient in many locations with the most notable speed maximum being near 0°E in Southern Hemisphere spring. The ten-year run block speed plot gives a clue to a major deficiency of the model climate. Almost the entire hemisphere at all seasons is dominated by highly transient blocking events (some of these might not be identified as blocks by a synoptician, but refer to the discussion of terminology in section 2). Looking at time–longitude plots of the individual easterly flow events and the way in which they are objectively grouped into blocks helps explain this behavior. Apparently the model produces eastward-propagating waves that are reflected in transient eastward-moving easterly flow events that are grouped into blocks. These events, while not entirely absent in the observed data, are more prevalent and of greater amplitude in the ten-year run.

Again, the Southern Hemisphere has been examined at 300, 500, and 700 mb and for a number of threshold values. Results are similar to those for the Northern Hemisphere. There is no obvious tilt with height of blocking events, and changing the threshold appears to produce little or no improvement in the ten-year results when compared with observations.

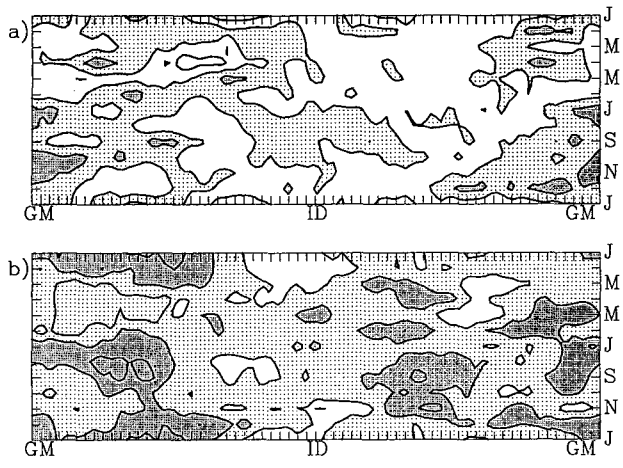

FIG. 8. Average eastward zonal velocity in degrees per day of (a) observed and (b) ten-year run Southern Hemisphere blocking events. Contour interval is 2.0 with light stippling for values exceeding 2.0 and dark stippling for values exceeding 4.0.

d. Conclusions

The blocking climatology of the Northern Hemisphere in the MRF ten-year run was found to be generally quite good. The model was able to reproduce the two largest centers of blocking activity at the appropriate time of year. It is clear that if other elements of the underlying climatology in the model run are conducive, the model is able to generate a reasonable number of blocking events and to persist them for extended periods as demonstrated again by the midwinter maxima over the Northern Hemisphere oceans (compare observed and ten-year run panels from Figs. 5 and 6). Nevertheless, the model is deficient in a number of ways. The MRF has too few Northern Hemisphere blocks except over the midwinter oceanic maxima, and those blocks that are produced are too weak.

In the Southern Hemisphere, the MRF climatology is much less satisfactory. Although a realistic number of short-lived blocks are produced, there are far too few persistent blocks. The geographical and seasonal distribution of the model blocks is only vaguely reminiscent of the observed patterns. The fact that the model has many unrealistically transient "blocking" events appears to be one of the major shortcomings in the Southern Hemisphere.

6. Evolution of forecast model errors

To this point, the climatology of blocking in the ten-year run of the MRF model has been compared to the observed climatology. An interesting question is how rapidly the climate of the model switches from the observed climate to the ten-year run climate as forecast lead time is increased from zero. This type of study has been performed previously with a number of models (Arpe and Klinker 1986; Sumi and Kanamitsu 1984; Surgi 1989), although not for lead times as great as those to be examined here. The climate drift in the MRF has also been demonstrated in several studies including Tracton et al. (1989).

In this section, a large number of long forecasts by the MRF model are used to examine the changes that take place in the distribution of easterly flow events as lead time is increased. Easterly flow events are used as a proxy for blocking because it is difficult to produce a fair comparison of blocking events from a relatively short time series (since long-lived blocks are unfairly excluded by the short duration of the dataset). The results in the two previous sections illustrate the strong relationship between individual easterly flow events and blocks.

a. DERF dataset

The dataset used is from the DERF90 experiment performed at the National Meteorological Center by S. Saha, E. Kalnay, M. Kanamitsu, and H. van den

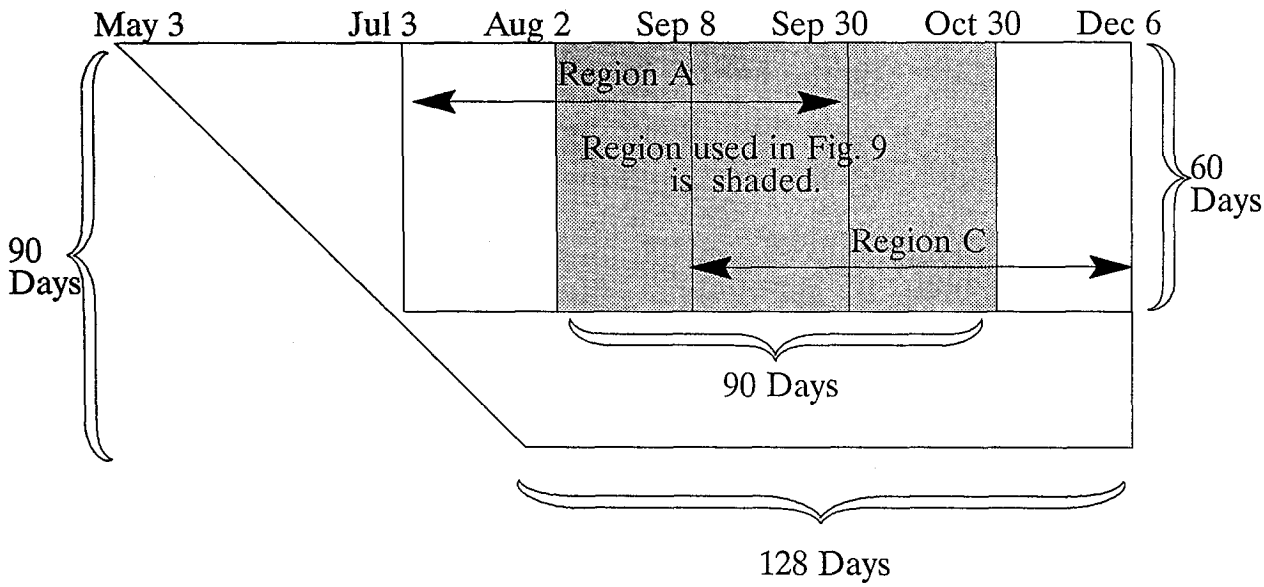

FIG. 9. Schematic diagram of the DERF90 dataset. The block of 90 60-day forecasts used in producing Fig. 10 is shaded. The regions marked A and C are the other two regions studied.

Dool. This dataset includes forecasts for lead times ranging from 1 to 90 days produced for a 128-day period starting on 3 May 1990. Forecasts for shorter lead times are included at the end of the 128 days to complete the dataset shown in Fig. 9.

The version of the MRF used for the DERF90 experiment is almost identical to that used for the ten-year run, but with slightly modified boundary conditions. The snow depth and soil moisture are interactive, but are attracted to an evolving climatology with a 90-day *e*-folding time. The sea ice distribution is set to the observed initial anomaly for 30 days, and the climatological distribution for longer leads. The SST begins with the initial observed fields and damps toward the climatology with a 90-day *e*-folding time.

The phenomenon of interest here is the way in which the distribution of blocking in the model evolves from the initial observed blocking climate to its own (ten-year run) climate at extended ranges. Previous studies of blocking climate drift have been limited to lead times of ten days (Tibaldi and Molteni 1990).

Figure 9 shows a schematic of the DERF90 dataset with forecast lead time increasing downward. In this study, three different 90-day blocks of forecasts with leads out to 60 days are examined. The results for the shaded region, starting on 2 August and ending on 30 October, are presented in Fig. 10; results for regions A and C are qualitatively similar. Forecasts out to 60 days are examined since the model blocking climate seems to be drifting significantly still past 30 days. It is desirable to make the number of forecasts in this dataset as large as possible to increase significance of the results but not so large that the results are smeared out by seasonal variations. For this reason, 90-day periods are selected.

The results for the shaded region in Fig. 9 are displayed in plots of easterly flow frequency as a function of longitude and forecast lead time (Fig. 10). In addition, short strips depicting the easterly flow frequency of the observed GDAS and ten-year run for the period 2 August through 30 October are attached to the top and bottom of the plots. The initial zero lead climate of the DERF90 run is similar to the GDAS climate, but of course not identical due to interannual variation. The extreme long lead forecasts from the DERF90 are similar to the ten-year run climate, but are not identical, this time due to the limited sample of forecasts and the differing external forcing of the DERF90 run. It is also conceivable that the initial conditions are still influencing the DERF climate, in some as yet unknown manner, even at lead times past 30 days (Michaud 1990).

b. Results

Figure 10a shows the Northern Hemisphere easterly flow frequency as a function of forecast lead time. There is a sharp decrease in the frequency during the first two days of the forecast, followed by a slower decline out to about day 14. This is similar to changes in other model quantities (Johansson et al. 1993) and to changes previously noted in forecasts of blocking in a variety of models (Tracton 1990; Tibaldi and Molteni 1990). By day 14 there are almost no easterly flow events in the model. It is this dearth of easterly flow events (and, hence, of blocking) that leads to the

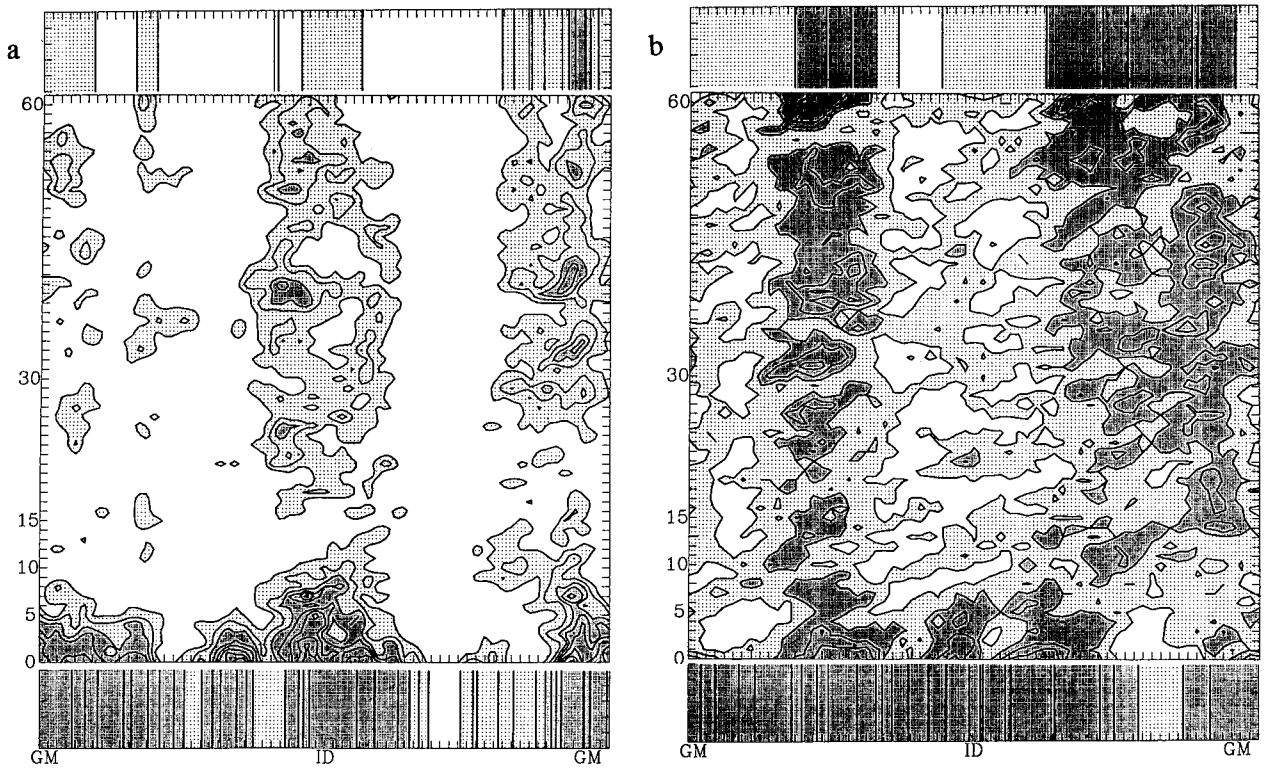

FIG. 10. Frequency of easterly flow events as a function of longitude and DERF90 forecast lead time for the (a) Northern Hemisphere and (b) Southern Hemisphere. The contour interval in (a) is 0.025 with light stippling for values exceeding 0.025 and dark stippling for values exceeding 0.075. In (b) the contour interval is 0.05 with light stippling for values exceeding 0.05 and dark stippling for values exceeding 0.10. The strips at the bottom are for the observed data from the same time of year as the DERF forecasts, while the top horizontal strips are the mean for the ten-year run from the same time of year.

MRF's difficulties in predicting blocking events at medium-range lead times. Tracton (1990) noted the same difficulty in predicting blocks in an older version of the MRF model. After day 14, new areas of higher frequency of easterly flow reappear, this time in the positions of the ten-year run climatological maxima. The rapid drop in easterly flow frequency with lead time during the first two days may be partially due to excessive damping in the model. However, the resurgence of easterly flow frequency at extended leads demonstrates that excessive damping is not the primary problem here.

Instead, this result suggests that in the Northern Hemisphere, at least for the T40 version of the MRF studied here, the climate drift of the model plays a significant role in the model's inability to predict blocks at medium ranges. Even in regions where the blocking frequency of the ten-year run model and observed climates is similar, differences in other aspects of the climate (for instance the mean positions of the jets and transient cyclones) appear to result in a transient period during which the model is unable to form or maintain blocks. Once the model reaches its own ten-year run climate, it is again able to produce blocks, but it seems likely that any realistic influence of the initial conditions has been destroyed by this time.

Figure 10b shows the easterly flow frequency plot for the Southern Hemisphere. Again, the observed easterly flow areas disappear extremely rapidly during the first two forecast days. By day 9 the frequency of easterly flow events has dropped substantially at all longitudes. Once again, areas of more frequent occurrence that are in agreement with the ten-year results appear after day 10. These changes appear to happen at somewhat shorter lead times in the Southern Hemisphere than in the Northern Hemisphere, but could still be symptoms of the same model deficiencies. The minimum in blocking in the Southern Hemisphere is not as drastic as that in the Northern Hemisphere.

c. Discussion of blocking climate drift

In order to extend the range of useful forecasts of blocking events, the model climatology must be made to more closely resemble the observed climate. Apparently, even if the observed and model climates of blocking are fairly similar regionally, as they are over the Atlantic in Fig. 10a, the model is unable to produce a smooth change from the observed to the model cli-

mate; hence, the dearth of easterly flow events at leads just past ten days.

One possible qualitative explanation of the medium-range minimum in MRF blocking frequency is presented here. In the observed Northern Hemisphere, the two largest regions of blocking are near the downstream sides of the two major jet streams. In fact, studies have suggested that blocks may develop as an instability of the time averaged basic state jets (Frederiksen 1983; Frederiksen and Bell 1987). Other studies have pointed out the possible role of smaller-scale baroclinic disturbances in the formation, maintenance, and destruction of blocks (Blackmon et al. 1986; Illari 1984).

It is a common feature of most NWP models and GCMs to produce zonally averaged midlatitude jet streams that are too strong and too far poleward (Arpe and Klinker 1986; Miyakoda et al. 1986); however, this problem has largely been corrected in the MRF (White and Caplan 1991; Caplan and White 1989). Nevertheless, the average strength and position of the zonally varying jets in the MRF shifts during the first ten days of the forecast period on the average.

Now, suppose a block exists in the observed atmosphere. The block's persistence is dependent on baroclinic instabilities of the associated jet. When the forecast model is integrated, the jet shifts, leaving the original block separated from the baroclinic systems that are prerequisite for its survival. Hence, all the original observed blocks decay, generally within the first few days. New blocks are unable to form as long as the jet position continues to shift. Once the jet has drifted to a more stationary position, baroclinic disturbances are able to form again. When these small synoptic-scale systems are available, blocks can be formed again, this time in the positions favored by the model's climatological jet.

There is some additional experimental evidence to support this hypothesis. The kinetic energy of the transient midlatitude flow, which is directly related to baroclinic synoptic systems, is found to fall off rapidly in the first few days of MRF forecasts, before rebounding somewhat at leads past ten days (Johannson et al. 1993). This is consistent with the idea of a transient jet being unable to produce baroclinic systems through instability as it moves to its model climatological position. Although the model kinetic energy does rebound after the transient period, it never reaches the levels found in the observations, possibly because of excessive damping used in forecast models. This reduced baroclinic activity might explain the reduced strength of the average model blocks (Chen 1989).

Figure 11 is provided to demonstrate the amount of drift found in the zonally varying MRF fields. The first panel displays the difference between the average of the 90 five-day lead forecasts verifying during the period from 2 August to 30 October and the 90 analyses verifying over the same period. Figures 11b and 11c display the same field but for 10- and 20-day lead MRF forecasts, respectively. Similar figures for longer lead forecasts (not shown) are all quite similar to the 20-day lead climate drift in Fig. 11c. The climate drift found in the DERF90 MRF run is apparently large enough to have significant effects on the position of the jets and the related instabilities. Figure 11d shows the difference between the February and January 500-mb height fields from the ten-year CDDB climate database (an average of observed heights from 1979 through 1988). The five-day lead climate drift has amplitudes about half as large as this monthly difference, while the 10- and 20-day drifts in Figs. 11b and 11c have amplitudes comparable to the monthly climate change. Since the observed higher-order moments of the January and February climates are known to differ significantly, it seems reasonable to assume that the climate drift in the DERF90 runs is also large enough to affect the model climatology of blocks and synoptic scale transient systems.

The results here are for the MRF at a T40 truncation. Tracton (1990) has suggested that higher-resolution versions of the MRF would produce superior forecasts of blocking. However, if this physical explanation is reasonable, it is likely that the same lack of blocks at medium range would occur in higher-resolution versions of the model unless the drift of the underlying model jets is reduced significantly. As long as the mean jet positions of the model drift away from the observed climate, even temporarily, the relation between baroclinic systems and blocks would be disrupted.

7. Summary and conclusions

The climatology of blocking events in a ten-year integration of a recent version of NMC's MRF forecast model has been presented and compared to an observed climate. In addition, the climate drift of midlatitude easterly flow events, a proxy for blocking events, in the MRF for lead times out to 60 days has been examined for a single season.

The MRF is found to produce a fairly reasonable representation of the blocking climatology of the Northern Hemisphere. Although the model is unable to produce blocks of the observed amplitude, the observed maxima of blocking over the wintertime oceans are reproduced. The Siberian maximum and some details of the summer observed blocking pattern are not reproduced. The model produces blocks that are too ephemeral compared to the observations, except in the wintertime blocking maxima.

In the Southern Hemisphere, the model produces a considerably less satisfactory representation of the observed blocking climate. The model produces too few blocks at all longitudes and seasons, and is unable to persist the blocks it does form.

Many previous studies that have only examined the first few days of NWP model forecasts have concluded

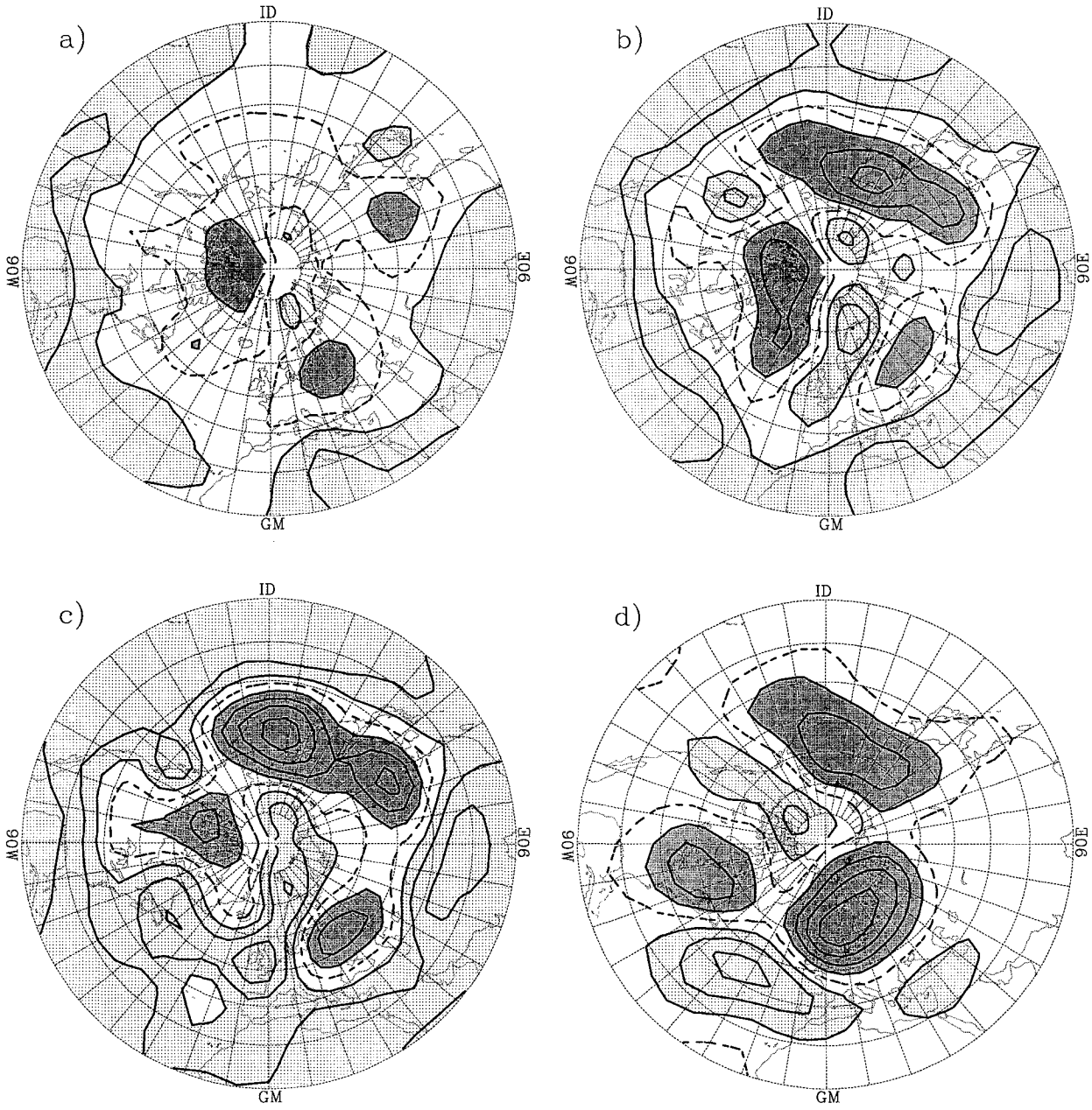

FIG. 11. Difference between the average of the analysis fields for 2 August to 30 October 1990, and the average of the DERF90 500-mb-height forecasts verifying over the same period for forecast leads of (a) 5 days, (b) 10 days, and (c) 20 days. The difference between 500-mb monthly climatologies for February and January are shown in (d). Contour interval is 20 m, the zero line is dashed, values greater than 20 m are heavily shaded while values less than −20 m are lightly shaded.

that these models are unable to produce or persist blocking events in a reasonable fashion. The results presented here demonstrate that the MRF climate can produce a large number of blocks and actually persists them longer than any observed blocks; this behavior is only found in the wintertime Northern Hemisphere maxima. Nevertheless, this suggests that more fundamental aspects of the model climate, for instance, the position of the midlatitude jets, are preventing the formation of the observed blocking distribution, rather than some inability of the model to form blocking events no matter what the underlying "basic" flow.

In the Southern Hemisphere, the model produces transient blocking events that are unlike those found in the Northern Hemisphere. The observed Southern Hemisphere appears to produce more transient events

than the Northern Hemisphere, but considerably fewer than are found in the ten-year run of the model. These transient blocking events need to be removed from the model's behavior if improved forecasts of Southern Hemisphere blocks are to be produced.

An examination of MRF forecasts of blocking frequency as a function of lead time shows that the number of blocks, initially distributed in a similar fashion to the observed climatology, drops rapidly during the first few days and reaches a minimum at leads near ten days. For lead times greater than ten days, the number of blocks increases again, this time with a distribution similar to the ten-year MRF climate. Significantly, this transition between the observed and model blocking climates is not smooth, even in regions where both climates have essentially identical distributions of blocking events.

The effects of the transition between the observed and model climate may partially explain the sharp drop in skill past about three days found in most MRF range forecasts. At lead times around ten days, the MRF is virtually unable to produce blocks; hence, it produces extremely poor forecasts during persistent observed blocking events. At lead times past ten days, the model is again able to produce blocks. If a block is formed in the model in the same approximate location as an observed block, a significant rebound of local forecast skill will be observed. It is important to note that this explanation implies that any return of skill is not useful, but simply represents the coincidence of the model and observed preferred blocking regions. It is conceivable that some useful skill does survive the medium-range minimum in blocking. One possibility is that anomalous boundary conditions in the model run impact the position of the resurgent blocks past ten days. It is also conceivable that some impact of the initial conditions might survive to the extended ranges. Further research is needed to determine if any of the extended range "skill" is useful.

Predicting blocking events is one of the primary goals of research into extended range forecasts. The results presented here argue that for the MRF, at least at the T40 resolution studied, the model climate drift makes the prediction of blocks past day 6 nearly impossible. A dynamical argument presented as a possible explanation of the inability to produce blocks at medium range is independent of resolution. As long as there is a climate drift in the underlying model jets, blocks might be expected to be rare during the transition between observed and model climates. In order to extend the range at which blocks can be predicted, the MRF must be modified in some fashion to reduce the climate drift at medium ranges. Initial studies in both simple models (Johansson and Saha 1989) and the MRF (Saha 1992) suggest that it may be possible to reduce climate drift substantially without modifying the details of the model physics and dynamics. Further research along these lines may be the most promising way to improve the forecast of blocking events.

Acknowledgments. The author is grateful to the many people at CAC and in NMC's Development Division who played a part in producing the ten-year and DERF90 runs of the MRF. Particular thanks are due to S. Saha for patient help in data acquisition and to H. van den Dool, J. Bell, and W. Ebisuzaki for their comments and encouragement. Thanks are also due to an anonymous reviewer and G. White for their thorough and constructive reviews of this paper.

REFERENCES

Arpe, K., and E. Klinker, 1986: Systematic errors of the ECMWF operational forecasting model in mid-latitudes. *Quart. J. Roy. Meteor. Soc.*, **112,** 181–202.

Barnston, A. G., and H. van den Dool, 1993: The structure and seasonality of the interannual standard deviation of monthly mean 700-mb height in the Northern Hemisphere. *J. Climate,* **6,** submitted.

Berberry, E. H., and M. N. Nuñez, 1989: An observational and numerical study of blocking episodes near South America. *J. Climate,* **2,** 1352–1361.

Blackmon, M. L., S. L. Mullen, and G. T. Bates, 1986: The climatology of blocking events in a perpetual January simulation of a spectral general circulation model. *J. Atmos. Sci.*, **43,** 1379–1405.

Caplan, P. M., and G. H. White, 1989: Performance of the National Meteorological Center's Medium-Range Model. *Wea. Forecasting,* **4,** 391–400.

Chen, T.-C., and J. Shukla, 1983: Diagnostic analysis and spectral energetics of a blocking event in the GLAS climate model simulation. *Mon. Wea. Rev.*, **111,** 3–22.

Chen, W. Y., 1989: Estimate of dynamical predictability from NMC DERF experiments. *Mon. Wea. Rev.*, **117,** 1228–1236.

Chervin, R. M., 1986: Interannual variability and seasonal climate predictability. *J. Atmos. Sci.*, **43,** 233–251.

Dole, R. M., and N. D. Gordon, 1983: Persistent anomalies of the extratropical Northern Hemisphere wintertime circulation: Geographical distribution and regional persistence characteristics. *Mon. Wea. Rev.*, **111,** 1567–1586.

Frederiksen, J. S., 1983: A unified three-dimensional instability theory of the onset of blocking and cyclogenesis. II: Teleconnection patterns. *J. Atmos. Sci.*, **40,** 2593–2609.

——, and R. C. Bell, 1987: Teleconnection patterns and the role of baroclinic, barotropic, and topographic instability. *J. Atmos. Sci.*, **44,** 2200–2218.

Hansen, A. R., and A. Sutera, 1991: Planetary-scale flow regimes in midlatitudes of the Southern Hemisphere. *J. Atmos. Sci.*, **48,** 952–964.

——, ——, and J. J. Tribbia, 1991: The relation of multiple flow regimes to the climatic error in general circulation models: Southern Hemisphere winter. *J. Atmos. Sci.*, **48,** 1329–1335.

Houghton, D. D., R. G. Gallimore, and L. M. Keller, 1991: Stability and variability in a coupled ocean–atmosphere climate model: Results of 100-year simulation. *J. Climate,* **4,** 557–577.

Illari, L., 1984: A diagnostic study of the potential vorticity in a warm blocking anticyclone. *J. Atmos. Sci.*, **41,** 3518–3526.

Johansson, A., and S. Saha, 1989: Simulation of systematic error effects and their reduction in a simple model of the atmosphere. *Mon. Wea. Rev.*, **117,** 1658–1675.

——, B. Reinhold, and S. Saha, 1993: Transient-induced climate drift. *J. Atmos. Sci.*, **50,** 1161–1172.

Kalnay, E., M. Kanamitsu, and W. E. Baker, 1990: The NMC global forecast system. *Bull. Amer. Meteor. Soc.*, **71,** 1410–1428.

Kanamitsu, M., 1989: Description of the NMC global data assimilation and forecast system. *Wea. Forecasting,* **4,** 335–342.

——, K. C. Mo, and E. Kalnay, 1990: Annual cycle integration of the NMC MRF model. *Mon. Wea. Rev.*, **118,** 2543–2567.

Lejenäs, H., and H. Økland, 1983: Characteristics of Northern Hemisphere blocking as determined from a long time series of observational data. *Tellus,* **35A,** 350–362.

Mak, M., 1991: Dynamics of an atmospheric blocking as deduced from its local energetics. *Quart. J. Roy. Meteor. Soc.*, **117,** 477–493.

Michaud, R., 1990: Extended memory of the initial conditions in long-range forecasts of the January 1983 atmospheric circulation. *J. Climate,* **3,** 461–482.

Miyakoda, K., J. Sirutis, and J. Ploshay, 1986: One-month forecast experiments—Without anomaly boundary forcings. *Mon. Wea. Rev.*, **114,** 2363–2401.

Mullen, S. L., 1986: The local balances of vorticity and heat for blocking anticyclones in a spectral general circulation model. *J. Atmos. Sci.*, **43,** 1406–1441.

——, 1989: Model experiments on the impact of Pacific sea surface temperature anomalies on blocking frequency. *J. Climate,* **2,** 997–1013.

Randel, W. J., and D. L. Williamson, 1990: A comparison of the climate simulated by the NCAR community climate model (CCM1:R15) with ECMWF analyses. *J. Climate,* **3,** 608–633.

Rex, D. F., 1950: Blocking action in the middle troposphere and its effect on regional climate. Part I: An aerological study of blocking action. *Tellus,* **2,** 196–211.

Saha, S., 1992: Response of the NMC MRF model to systematic-error correction within integration. *Mon. Wea. Rev.*, **120,** 345–360.

Shukla, J., and K. C. Mo, 1983: Seasonal and geographic variation of blocking. *Mon. Wea. Rev.*, **111,** 388–402.

Sumi, A., and M. Kanamitsu, 1984: A study of systematic errors in a numerical weather prediction model. Part I: General aspects of the systematic errors and their relation with the transient eddies. *J. Meteor. Soc. Japan,* **62,** 234–251.

Surgi, N., 1989: Systematic errors of the FSU global spectral model. *Mon. Wea. Rev.*, **117,** 1751–1766.

Tibaldi, S., and F. Molteni, 1990: On the operational prediction of blocking. *Tellus,* **42A,** 343–365.

Tracton, S., 1990: Predictability and its relationship to scale interaction processes in blocking. *Mon. Wea. Rev.*, **118,** 1666–1695.

——, K. Mo, W. Chen, E. Kalnay, R. Kistler, and G. White, 1989: Dynamic extended range forecasting (DERF) at the National Meteorological Center. *Mon. Wea. Rev.*, **117,** 1604–1635.

Trenberth, K. E., 1991: Storm tracks in the Southern Hemisphere. *J. Atmos. Sci.*, **48,** 2159–2178.

——, and K. C. Mo, 1985: Blocking in the Southern Hemisphere. *Mon. Wea. Rev.*, **113,** 3–21.

Van den Dool, H. M., and S. Saha, 1993: Seasonal redistribution of atmospheric mass in a GCM. *J. Climate,* **6,** 22–30.

——, ——, and Z. Toth, 1991: The climate in a multi-year NMC model run. *Proc. Fifth Conf. on Climate Variations,* Denver, Amer. Meteor. Soc., 511–514.

White, G. H., and P. M. Caplan, 1991: Systematic Performance of the NMC Medium-Range Model. *Proc. Ninth Conf. on Numerical Weather Prediction,* Boulder, Amer. Meteor. Soc., 806–809.

Xu, J.-S., H. von Storch, and H. van Loon, 1990: The performance of four spectral GCMs in the Southern Hemisphere: The January and July climatology of the semiannual wave. *J. Climate,* **3,** 53–70.